arXiv:1209.5824v1 [cond-mat.quant-gas] 26 Sep 2012

Inverse Energy Cascade in Forced 2D Quantum Turbulence

Matthew T. Reeves,[1] Thomas P. Billam,[1] Brian P. Anderson,[2] and Ashton S. Bradley[1]
[1] *Jack Dodd Centre for Quantum Technology, Department of Physics, University of Otago, Dunedin 9016, New Zealand*
[2] *College of Optical Sciences, University of Arizona, Tucson, AZ 85721, USA*

We demonstrate an inverse energy cascade in a minimal model of forced 2D quantum vortex turbulence. We simulate the Gross-Pitaevskii equation for a moving superfluid subject to forcing by a stationary grid of obstacle potentials, and damping by a stationary thermal cloud. The forcing injects large amounts of vortex energy into the system at the scale of a few healing lengths. A regime of forcing and damping is identified where vortex energy is efficiently transported to large length scales via an inverse energy cascade associated with the growth of clusters of same-circulation vortices, a Kolmogorov scaling law in the kinetic energy spectrum over a substantial inertial range, and spectral condensation of kinetic energy at the scale of the system size. Our results provide clear evidence that the inverse energy cascade phenomenon, previously observed in a diverse range of classical systems, can also occur in quantum fluids.

Turbulent fluid flows are characterized by the conserved transfer of kinetic energy across length scales [1]. In classical 3D turbulence, large-scale forcing leads to a cascade of energy and vorticity towards smaller scales [2]. In stark contrast, small-scale forcing in 2D fluids may lead to an *inverse* energy cascade (IEC) [3, 4], associated with energy flux towards larger scales, and the emergence of macroscopic rotating structures from the turbulent flow. The IEC has been widely studied in classical fluids [2, 5] and observed over a large range of scales, from soap films [6, 7] to planetary atmospheres [8]. The IEC in classical fluids can be studied via a point-vortex model in which the growth of large-scale flows corresponds to the clustering of point-vortices with the same circulation [9, 10]. This model provides a link between classical and quantum turbulence (QT), and suggests the intriguing possibility that the IEC may be observable in quantum fluids. The possibility to realize effectively 2D superfluid flows has motivated the study of 2DQT in atomic Bose-Einstein condensates (BECs) [11–22], and such flows have been experimentally demonstrated [23, 24]. Although intermittent few-vortex clustering has been observed in the breakdown of superfluid flow around an obstacle [16, 23], establishment of a steady, large-scale IEC in a BEC is hindered by the compressibility of the superfluid, which allows vortex-antivortex annihilation [14, 15], and a direct cascade of acoustic energy via weak-wave turbulence [12].

In this Letter we demonstrate an IEC of quantum vortices in numerical simulations of a forced, damped BEC. We show that the interplay between the effects of forcing and damping leads to a regime where a clear IEC occurs. We analyze the dynamics of the 2DQT via the *incompressible* kinetic energy (IKE) spectrum [15, 25] associated with vortices, and the statistics of vortex clustering as identified by a cluster-finding algorithm. We observe three clear signatures of an IEC: (1) a sustained increase in the charge and spatial scale of vortex clusters; (2) a Kolmogorov $k^{-5/3}$ IKE spectrum [25] spanning an inertial range of up to 1.5 decades; and (3) spectral condensation [26] – a macroscopic accumulation of IKE at the largest length scales of the system.

Our system constitutes a BEC analog of forced 2D *grid turbulence*, a scenario that has been used to demonstrate the IEC in classical fluids [7]. We consider a superfluid moving with initial speed v that is stirred by a stationary, regularly-spaced grid of four narrow Gaussian potentials. We model the dynamics of the condensate, described by wavefunction $\psi(\mathbf{r}, t)$, using the damped Gross-Pitaevskii equation (dGPE) [27]

$$i\hbar\frac{\partial\psi(\mathbf{r},t)}{\partial t} = (1 - i\gamma)(\mathcal{L} - \mu)\psi(\mathbf{r}, t). \tag{1}$$

The operator $\mathcal{L}$ generates the zero-temperature GPE evolution, and for a quasi-2D BEC subject to tight harmonic confinement in the z-direction (with harmonic oscillator length l_z) can be written as

$$\mathcal{L} = -\frac{\hbar^2\nabla_\perp^2}{2m} + V(x, y) + g_2|\psi(x, y, t)|^2, \tag{2}$$

where $V(x, y)$ is the grid potential, and $g_2 = 2\sqrt{2\pi}\hbar^2 a_s/ml_z$, for atoms of mass m interacting with s-wave scattering length a_s. Dissipative collisions between condensate atoms and a stationary thermal cloud at chemical potential μ are described by the dimensionless damping rate γ. Imposing periodic boundary conditions, our system provides a model of the obstacle-induced spin-down of a persistent current immersed in a stationary thermal cloud [28].

We work in energy, length and time units of chemical potential μ, healing length $\xi = \hbar/mc$, and ξ/c respectively, where $c = \sqrt{\mu/m}$ is the speed of sound in the homogeneous system. We numerically solve the dGPE in a periodic box of length $L = 512\xi$, for time $t = 800\xi/c$ (at which time the turbulent wake reaches $x = L/2$). To eliminate the transient effects of abruptly raising the grid potential we begin from a ground state of the dGPE where the grid is co-moving with the flow, and stop the grid motion at $t = 0$. The grid potentials are then located at $x = -L/2 + 8\xi$ and equally spaced by $L/4$ in the y direction. We add a small amount of initial noise to break the symmetry, and collect statistical information about the flow by computing multiple trajectories. Typical vortex configurations of the system at time $t = 700\xi/c$ are shown in Fig. 1. To observe turbulent flow, we choose sufficiently high v $\approx 0.822c$ such that the grid nucleates vortices in a chaotic manner [16], rather than periodically [29]. To optimize vortex injection, we choose grid potential height $V_0 = 100\mu$ and $1/e^2$

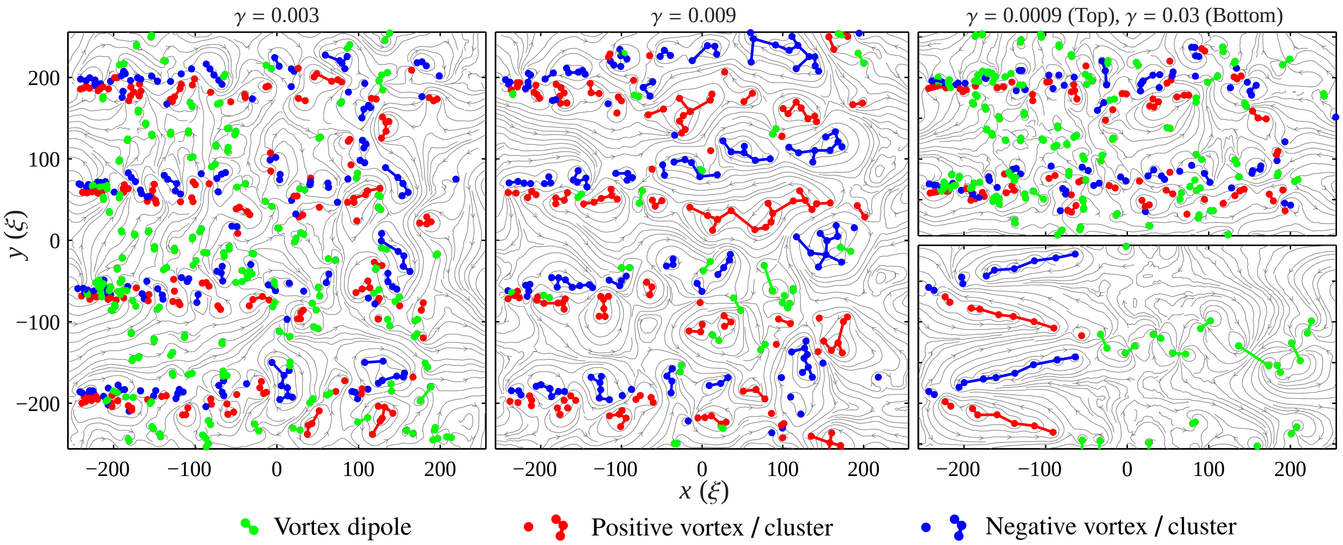

FIG. 1. (Color online) Vortex configurations in a rightward-flowing superfluid stirred by a stationary grid of obstacle potentials, located at the left. Dots indicate the locations of positive (counter-clockwise circulation) and negative (clockwise circulation) vortices at time $t = 700\xi/c$. The vortices have been sorted into dipoles, free vortices, and clusters (see legend) using the cluster-finding algorithm (see text). Vortices in dipoles at the smallest length scales are not resolvable on the scale shown, and appear as isolated green dots. Streamlines (grey lines) give a visualization of the vortex-only velocity field by constructing the velocity field of an identical configuration of point vortices.

radius $w_0 = \sqrt{8}\xi$. Each obstacle potential injects streams of opposite-signed vortices separated by distance $\sim 2w_0$. As the linear momentum of a dipole is proportional to the vortex separation, these streams carry negative momentum, arresting the superflow.

The dimensionless damping rate γ influences the vortex dynamics, and can be controlled via the temperature. In *decaying* 2DQT, damping assists dipole recombination, and thus transfers IKE to small length scales via a direct energy cascade [15]. In our forced system damping is vital for generating an IEC. At low damping (Fig. 1, upper right panel), the vortex dynamics are dominated by mixing of the streams of opposite-sign vortices nucleated at each obstacle potential, leading to dipole annihilation. In contrast, high damping (Fig. 1, lower right panel) acts to reduce the linear momentum of the condensate by rapidly polarizing (spatially separating) the vortex streams. This suppresses dipole annihilation until streams from adjacent obstacles merge. Intermediate damping (Fig. 1, center panel) leads instead to the formation of small clusters of like-sign vortices. The subsequent merging and expansion of these clusters, ultimately leading to macroscopic dipoles approaching the scale of the system, is the spatial signature of an IEC in 2DQT [21].

To quantify the vortex clustering seen in Fig. 1 we have developed a cluster-finding algorithm that identifies the vortex clusters within a given configuration. This yields more detailed spatio-temporal statistical information regarding vortex clustering than scalar measures [22]. The algorithm consists of two rules: (1) *Opposite-sign vortices that are mutual nearest-neighbors constitute a dipole and are removed from the algorithm's consideration*. (2) *Same-sign vortices that are closer to each other than either is to an opposite-sign vortex are placed in the same cluster*. Rule 1 (2) is applied recursively to all vortices still under consideration until no more vortices can be added to dipoles (clusters). Rule 1 is applied first, removing the short-range velocity fields of dipoles. The algorithm yields a decomposition of the configuration into clusters, dipoles, and free vortices that corresponds extremely well to the streamlines of the point-vortex velocity field, as seen in Fig. 1.

In Fig. 2 we show the mean charge (number of vortices), κ_c, and radius (average distance of vortices from the cluster center), r_c, of all clusters within a sample box of size $(64\xi,512\xi)$. For each of the four values of γ, we combine statistics from eight trajectories. In Fig. 2(a) we analyze the configurations at time $t = 700\xi/c$ by centering the sampling box at $(d - L/2,0)$, where d is the downstream distance from the grid. In Fig. 2(b) we analyze the configurations as a function of time, centering the sample box at $(\mathrm{v}t - 32\xi,0)$ [inset $(\mathrm{v}t - 96\xi,0)$] such that it is co-moving with the flow. The results of these two analysis methods are in reasonable quantitative agreement, indicating that the frozen-turbulence approximation (equivalence of d and $\mathrm{v}t$) is satisfied [4]. The strong increases in κ_c and r_c over large ranges of d and t in the case $\gamma = 0.009$ are a clear signature of an IEC. For lower values of the damping ($\gamma = 0.003$ and $\gamma = 0.0009$) κ_c remains generally constant while r_c increases slowly, suggesting the IEC is weak if present. For higher damping ($\gamma = 0.03$) an initial rapid increase in κ_c, r_c is followed by a similarly rapid decrease in both quantities; this is consistent with a strong IEC immediately behind the grid,

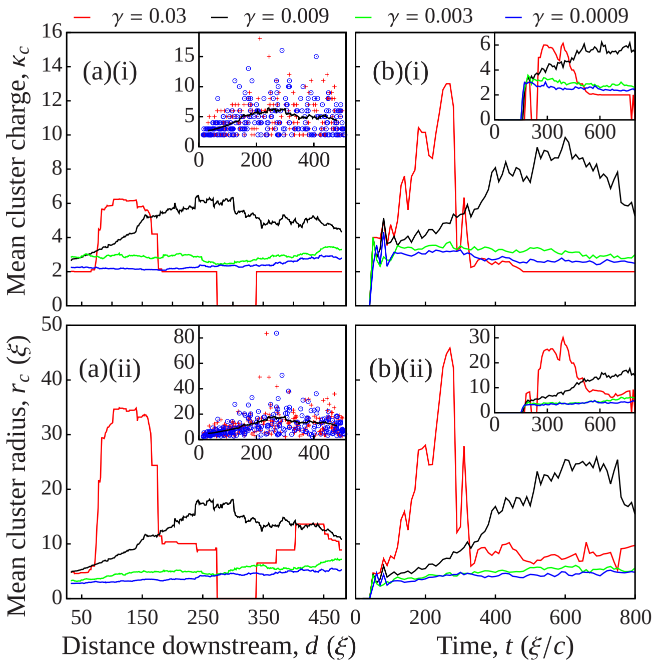

FIG. 2. (Color online) Spatio-temporal statistics of vortex clustering. For four values of γ we show the mean charge, κ_c, and radius, r_c, of clusters identified by the cluster-finding algorithm with cluster center located in a box of dimensions (64ξ,512ξ), averaged over eight trajectories. Both quantities are shown as a function of: (a) downstream distance from the grid, d, using a box centered at $(d - L/2, 0)$ at time $t = 700\xi/c$; (b) time, t, using a box centered at $(vt - 32\xi, 0)$ and hence co-moving with the flow. Insets show: (a) distribution of positive (red plus) and negative (blue circle) clusters for the case $\gamma = 0.009$; (b) κ_c and r_c for a box centered at $(vt - 96\xi, 0)$. By definition the smallest clusters consist of 2 vortices.

which is destroyed by dipole recombination when the streams meet (Fig. 1).

The IKE spectrum of our system (Fig. 3) can be compared to the spectrum for an *ideal* model of 2DQT given in Ref. [21]. This model consists of quantum vortices with compressible cores; incompressible energy is efficiently transported from small-scale forcing towards large scales via vortex dynamics, but coupling of vortex dynamics to the sound field is neglected. In the ultraviolet (UV) region ($k \gg \xi^{-1}$) the IKE spectrum is

$$E^i_U(k) = C(k\xi)^{-3} \equiv \Lambda^2 N\Omega\xi^3(k\xi)^{-3}, \tag{3}$$

where Λ is a dimensionless constant related to the structure of a compressible quantum vortex core, N is the total vortex number, $\Omega = 2\pi\hbar^2 n_0/m\xi^2$ is a constant with dimensions of enstrophy, and $n_0 = \mu/g_2$ is the homogenous system density. The k^{-3} form of Eq. (3) is a universal feature of compressible 2DQT arising from the finite size of a vortex core, and is not associated with a direct enstrophy cascade. At the wave number $\bar{k} \equiv \xi^{-1}$ there is a cross-over to point-vortex behavior in the infrared (IR) region ($L^{-1} \lesssim k \lesssim \bar{k}$). Assuming (a) forcing wavenumber $k_f \approx \bar{k}$, and (b) all N vortices participate in clustering, the IR-region spectrum takes the Kolmogorov form

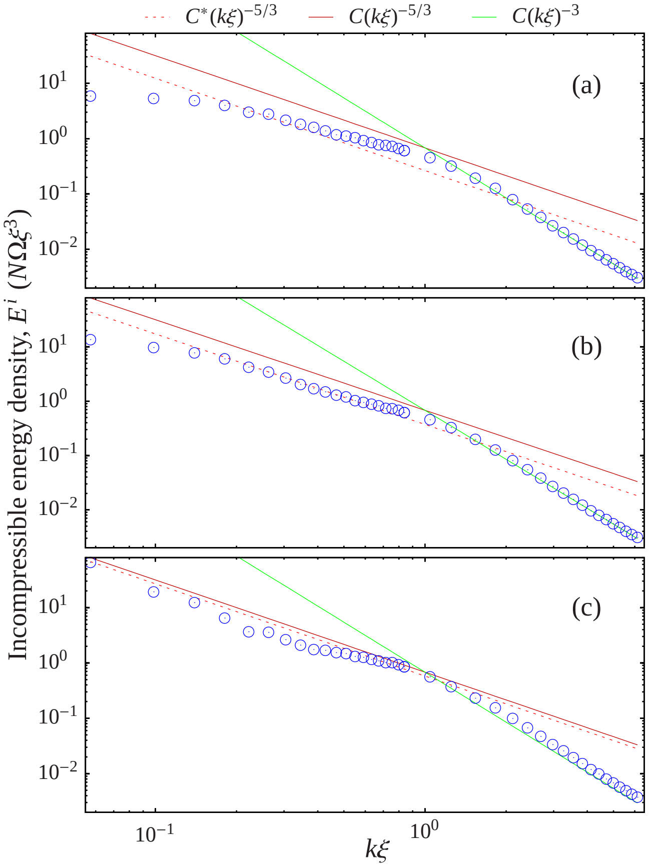

FIG. 3. (Color online) Incompressible kinetic energy spectra at $t = 550\xi/c$ for damping parameters (a) $\gamma = 0.0009$ (b) $\gamma = 0.003$ (c) $\gamma = 0.009$ (circles), averaged over eight trajectories. Lines show theoretical predictions for k^{-3} [Eq. (3)] and Kolmogorov $k^{-5/3}$ [Eq. (4)] spectra (see legend) in ideal 2DQT, with no fitted parameters. The Kolmogorov spectrum is shown using both the clustered vortex number N_c (constant C^*), and the total vortex number N (constant C) for comparison.

$$E^i_C(k) = C(k\xi)^{-5/3} \tag{4}$$

over an inertial range. The extent of the inertial range is linked to the scale range of vortex clusters, and it has been shown that appropriately distributed vortices in clusters of charge $\kappa_c = 5$ are sufficient to generate a decade of inertial range. In our simulations k_f is determined by w_0: treating the injected vortices as streams of dipoles of width $l_f = 2w_0$, forcing occurs near $k_f = 2\pi/l_f$, corresponding to the peak in the IKE spectrum of such a vortex dipole [21]. Our choice $w_0 = \sqrt{8}\xi$ thus corresponds to $k_f = 1.11\bar{k}$, satisfying assumption (a). Since the number of vortices participating in clustering, N_c, is generally less than N, assumption (b) is not always satisfied. However, in this case the replacements $N \rightarrow N_c$ and $C \rightarrow C^* \equiv CN_c/N$ in Eq. (4) give a better description of the inertial range, while retaining continuity with the UV region at $k \approx \bar{k}$.

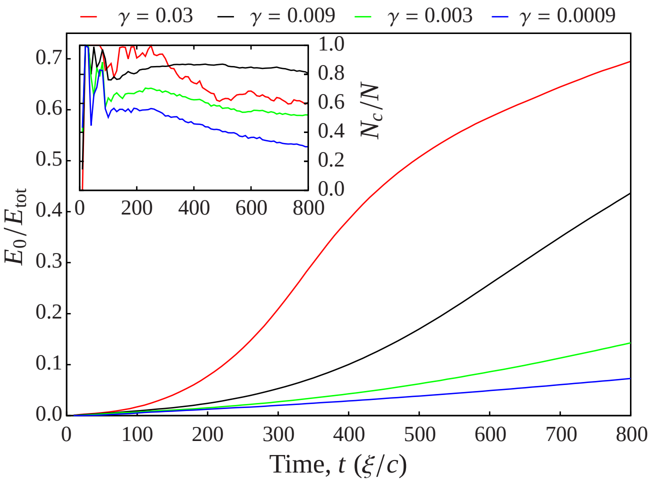

FIG. 4. (Color online) Fraction of the total kinetic energy, $E_{\rm tot}$, stored as incompressible kinetic energy at scale L (E_0, see text), as a function of time. Inset: Vortex clustered fraction as a function of time.

For all values of damping the UV spectrum agrees with the 2DQT prediction [Eq. (3)]. For $\gamma = 0.0009$ [Fig. 3(a)] the IR spectrum does not exhibit a clear $k^{-5/3}$ scaling and lacks temporal stability. A buildup of energy around $\bar{k}$ is evident, suggesting a possible *bottleneck* [30], associated with inefficient energy transport away from forcing wavenumber k_f. For $\gamma = 0.003$ [Fig. 3(b)] the IR spectrum closely follows the modified 2DQT prediction [Eq. (4) with $N \to N_c$] over an inertial range of around a decade of k, is steady for times $300\xi/c \lesssim t \lesssim 600\xi/c$, and has a weaker bottleneck around k_f. This is consistent with increased vortex clustering (Fig. 1), and the onset of an IEC. For $\gamma = 0.009$ [Fig. 3(c)], the IR spectrum approximates the ideal 2DQT form [Eq. (4)] over a wide inertial range ($\sim$ 1.5 decades) and is completely stable after $t \approx 400\xi/c$. This is consistent with strong vortex clustering (Fig. 1), and a fully developed IEC. For strong damping ($\gamma = 0.03$) the spectrum remains qualitatively similar, although agreement with the ideal 2DQT IKE spectrum prediction is degraded by the abrupt surge in dipole annihilation occurring when vortex streams from adjacent obstacle potentials meet (Fig. 1).

Flux of IKE to scales approaching the system size leads to an effect known as *spectral condensation*, associated with the emergence of macroscopic rotating structures [26]. Previously, IKE fluxes in compressible, forced 2DQT have been calculated by neglecting the compressible part of the kinetic energy, or introducing assumptions regarding its coupling to the IKE spectrum [14, 15]. Here we provide a clear demonstration of a negative IKE flux by considering the ratio of the IKE in mode $k = 0$, given by $E_0 \equiv E^i(k = 0)\Delta k$ (where $\Delta k = 2\pi/L$), to the total kinetic energy, $E_{\rm tot} = (\hbar^2/2m)\int d^2\mathbf{r}\,|\nabla_\perp\psi(\mathbf{r})|^2$. We eliminate the contribution of the initial superflow to the IKE by computing the energies in the frame co-moving with the condensate at $t = 0$ (Fig. 4). For weak damping ($\gamma = 0.0009$ and $\gamma = 0.003$) the ratio $E_0/E_{\rm tot}$ remains small. However, for higher damping ($\gamma = 0.009$ and $\gamma = 0.03$) the ratio $E_0/E_{\rm tot}$ initially grows rapidly, leading to significant spectral condensation. Merging of the vortex streams at later times (Fig. 1) slows this growth (most notably for $\gamma = 0.03$) and leads to a decline in the clustered fraction in all cases except for $\gamma = 0.009$, where it remains consistently high (Fig. 4, inset). Since the fractional occupation of the ground-state remains below 10^{-4}, this spectral condensation is not due to Bose-Einstein condensation into the ground-state, but rather emerges from macroscopic vortex clustering.

We have demonstrated an inverse energy cascade in a quantum analog of classical 2D grid turbulence [7]. We solve the Gross-Pitaevskii equation describing a moving superfluid arrested by a grid of obstacle potentials, and damped by a stationary thermal cloud. An inverse energy cascade is identified via the growth and expansion of vortex clusters, a Kolmogorov $k^{-5/3}$ incompressible kinetic energy spectrum, and a flux of incompressible kinetic energy to large scales. The demonstration of an inverse energy cascade of quantum vortices in a minimal model establishes a new link between classical and quantum turbulence, and our methods of analysis form a foundation for future studies of quantum vortex turbulence in two dimensional superfluids. Our findings open new directions in the study of forced and decaying superfluid turbulence [16, 29] and provide a dynamical realization of the negative-temperature states for point vortices originally envisaged by Onsager [31].

This research was supported by the US National Science Foundation (PHY-1205713), The Marsden Fund of New Zealand (UOO162), and The Royal Society of New Zealand (UOO004).

[1] A. N. Kolmogorov, Dokl. Akad. Nauk. SSSR **30**, 301 (1941).
[2] K. Sreenivasan, Rev. Mod Phys. **71**, S383 (1999).
[3] R. H. Kraichnan and D. Montgomery, Rep. Prog. Phys. **43**, 547 (1980).
[4] U. Frisch, *Turbulence: The Legacy of A. N. Kolmogorov* (Cambridge University Press, The Pitt Building, Trumpington Street, Cambridge CB2 1RP, 1995).
[5] G. Boffetta and R. E. Ecke, Annu. Rev. Fluid Mech. **44**, 427 (2012).
[6] B. K. Martin, X. L. Wu, W. I. Goldburg, and M. A. Rutgers, Phys. Rev. Lett. **80**, 3964 (1998).
[7] M. Rutgers, Phys. Rev. Lett. **81**, 2244 (1998).
[8] F. Bouchet and J. Sommeria, J. Fluid Mech. **464**, 165 (2002).
[9] G. Eyink and K. R. Sreenivasan, Rev. Mod. Phys. **78**, 87 (2006).
[10] E. D. Siggia and H. Aref, Phys. Fluids **24**, 171 (1981).
[11] N. G. Parker and C. S. Adams, Phys. Rev. Lett. **95**, 145301 (2005).
[12] S. Nazarenko and M. Onorato, J. Low Temp. Phys. **146**, 31 (2007).
[13] T. L. Horng *et al.*, Phys. Rev. A **80**, 023618 (2009).
[14] R. Numasato and M. Tsubota, J. Low Temp. Phys. **158**, 415 (2010).
[15] R. Numasato, M. Tsubota, and V. S. L'vov, Phys. Rev. A **81**,

063630 (2010).

[16] K. Sasaki, N. Suzuki, and H. Saito, Phys. Rev. Lett. **104**, 150404 (2010).

[17] A. C. White *et al.*, Phys. Rev. Lett. **104**, 075301 (2010).

[18] B. Nowak, D. Sexty, and T. Gasenzer, Phys. Rev. B **84**, 020506 (2011).

[19] B. Nowak, J. Schole, D. Sexty, and T. Gasenzer, Phys. Rev. A **85**, 043627 (2012).

[20] J. Schole, B. Nowak, and T. Gasenzer, Phys. Rev. A **86**, 013624 (2012).

[21] A. S. Bradley and B. P. Anderson, Energy spectra of vortex distributions in two-dimensional quantum turbulence, arXiv:1204.1103, 2012.

[22] A. White, C. Barenghi, and N. Proukakis, Phys. Rev. A **86**, 013635 (2012).

[23] T. W. Neely *et al.*, Phys. Rev. Lett. **104**, 160401 (2010).

[24] T. W. Neely *et al.*, Characteristics of Two-Dimensional Quantum Turbulence in a Compressible Superfluid, arXiv:1204.1102, 2012.

[25] C. Nore, M. Abid, and M. Brachet, Phys. Rev. Lett. **78**, 3896 (1997).

[26] M. Chertkov, C. Connaughton, I. Kolokolov, and V. Lebedev, Phys. Rev. Lett. **99**, 084501 (2007).

[27] P. B. Blakie *et al.*, Adv. in Phys. **57**, 363 (2008).

[28] A. Ramanathan *et al.*, Phys. Rev. Lett. **106**, 130401 (2011).

[29] T. Frisch, Y. Pomeau, and S. Rica, Phys. Rev. Lett. **69**, 1644 (1992).

[30] V. L'vov, S. Nazarenko, and O. Rudenko, Phys. Rev. B **76**, 024520 (2007).

[31] G. L. Eyink and K. R. Sreenivasan, Rev. Mod. Phys. **78**, 87 (2006).